Journal of Power Sources 180 (2008) 195–198

Contents lists available at ScienceDirect

Journal of Power Sources

journal homepage: www.elsevier.com/locate/jpowsour

Short communication

Thick-film electrolyte (thickness <20 μm)-supported solid oxide fuel cells

Jong Hoon Joo, Gyeong Man Choi*

Fuel Cell Research Center and Department of Materials Science and Engineering, Pohang University of Science and Technology, Pohang 790-784, Republic of Korea

ARTICLE INFO

Article history:
Received 17 October 2007
Accepted 4 February 2008
Available online 16 February 2008

Keywords:
Solid oxide fuel cell
Self-supporting thick film electrolyte
Yttria-stabilized zirconia
Cell performance
Power density

ABSTRACT

A novel design of solid oxide fuel cell (SOFC) which utilizes a thick film (<20 μm) as an electrolyte support is developed and tested. The sintered 16 μm-thick yttria-stabilized zirconia (YSZ) electrolyte film is mounted on a 1-mm thick YSZ ring by sintering the two pieces together. With this new configuration, it is possible to fabricate a thick (<20 μm) electrolyte-supported SOFC and measure the power density of the unit cell. With LSCF ($La_{0.6}Sr_{0.4}Co_{0.2}Fe_{0.8}O_{3-\delta}$) as a cathode and Ni–YSZ as a composite anode, the cell with a 16 μm-thick YSZ electrolyte achieves a high performance, i.e., a maximum power density of 590 mW cm^{-2} at 800 °C. This value is comparable with that of most anode-supported SOFCs using YSZ electrolytes.

1. Introduction

Fuel cell is an energy conversion device that generates electricity and heat by electrochemically combining a gaseous fuel and an oxidizing gas via an ion-conducting electrolyte. Energy conversion using solid oxide fuel cells (SOFCs) is highly efficient and environmental friendly, with low emissions of NO_x, dust, and noise. In addition, SOFCs offer flexibility in fuel selection (coal gas, hydrogen, etc.). The SOFC unit cell is composed of three components: electrolyte, cathode and anode [1,2]. Most of the development has focused on planar or tubular designs of SOFCs. In planar SOFCs, the cell components are configured as flat plates that are connected in electrical series. Planar SOFCs can be classified into two broad categories: an electrolyte-supported cell and an electrode-supported cell.

Conventionally, electrolyte-supported SOFCs use the electrolyte to support thin electrodes on either surface [3,4]. The advantages of this configuration are relatively strong structural support from a dense electrolyte and little susceptibility to a failure due to anode re-oxidation. In an anode-supported cell, the thin electrolyte layer cracks due to the volume change and sintering of the supporting anode accompanied by the Ni oxidation [5]. However, the electrolyte-supported structure limits the minimum electrolyte thickness to ~150 μm and thereby an operating temperature of about 900–1000 °C is required to minimize the high-ohmic loss due to the thick electrolyte [6]. Such a high temperature implies poor long-term stability and high-material costs, particularly for the interconnect materials. The high-temperature limits the choice of interconnect materials to a few ceramics that are thermally stable but expensive. Thus, lowering the operating temperature to 600–800 °C invokes many advantages. Low-cost metallic materials, e.g., ferritic stainless steels, can be used as interconnects. This makes the stack cheaper and more robust [4]. On the other hand, as the temperature is lowered, the ohmic loss across the solid electrolyte increases. This can be overcome by decreasing the thickness of electrolyte. In the case of a supported film electrolyte, a thickness of 5–30 μm is often possible.

Electrode-supported SOFCs with thin electrolytes can operate at reduced temperatures (600–800 °C). The most common example is the anode-supported SOFC. However, the disadvantages of this configuration include a mass-transport limitation due to the thick (e.g., 1 mm) electrode. In addition, to form a dense electrolyte and a porous anode, a careful co-sintering process has to be adopted. As a result, the whole process is both complex and time-consuming [7].

This study presents a thick film electrolyte (thickness <20 μm)-supported SOFC. The structure offers the advantages of both the electrolyte-supported and the electrode-supported design. Although a YSZ electrolyte thicker than 100 μm can be self-supporting, an electrolyte below 20 μm in thickness easily cracks in the self-supporting mode during the sealing procedure. Thus a new method has been developed for a thin electrolyte with a thickness of less than 20 μm. A ~16-μm thick YSZ electrolyte is mounted on 1-mm thick YSZ ring by sintering the two pieces together [8]. With this new configuration, it is possible to construct an electrolyte-supported SOFC and measure its power density. The electrochemical performance of a single cell based on the YSZ film is presented and discussed. The test reveals that it is possible to fabricate a thick-film electrolyte-supported SOFC.

* Corresponding author. Tel.: +82 54 279 2146; fax: +82 54 279 2399.
E-mail address: gmchoi@postech.ac.kr (G.M. Choi).

0378-7753/$ – see front matter © 2008 Elsevier B.V. All rights reserved.
doi:10.1016/j.jpowsour.2008.02.013

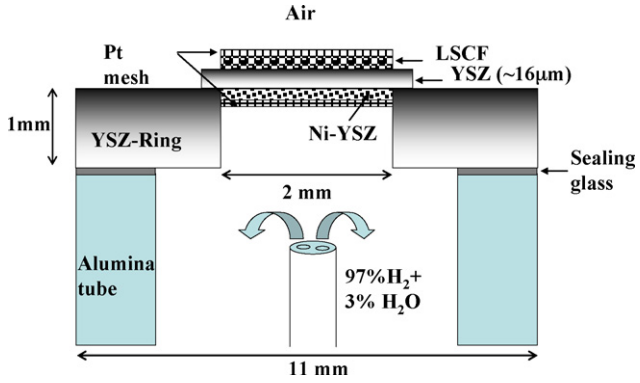

Fig. 1. Schematic illustration of the experimental set up for thin-film electrolyte-supported SOFCs.

2. Experimental procedure

In order to fabricate a free-standing YSZ film, commercial YSZ tape (8 mol% yttria-stabilized zirconia, Fuel Cell Store, USA) was cut in a desired shape and then sintered at 1550 °C for 3 h in air. The dense YSZ electrolyte had a thickness of ~16 μm after sintering. The relative sintered density was more than 95%, as estimated from the sample weight and dimension. The 16-μm thick YSZ electrolyte was mounted on a 1-mm thick YSZ cylindrical-ring (o.d. = 11 mm, i.d. = 2 mm) by using YSZ paste and sintering the two pieces together at 1400 °C for 3 h in air. YSZ paste was prepared by mixing YSZ powder (TZ-8YS, Tosoh, Japan) with an organic solution of α-terpineol and ethyl cellulose in a weight ratio of 10:1. The viscosity of the solution was controlled by adding di-ethylene glycol butyl ether. The organic solution was also used to prepare slurries for the cathode and the anode. A schematic diagram of the measurement cell is shown in Fig. 1. After mounting the YSZ film on the YSZ ring, a NiO–YSZ slurry was brush painted on the bottom surface of the supporting YSZ electrolyte and subsequently sintered at 1300 °C for 3 h in air. The NiO (Kojundo Chemical, Japan)–YSZ (TZ-8YS, Tosoh, Japan) (4:6 weight ratio) composite slurry was prepared by mixing the composite powder with the organic solution. In our previous study [9], the NiO–YSZ composite anode showed the best performance when sintered at 1300 °C. LSCF ($La_{0.6}Sr_{0.4}Co_{0.2}Fe_{0.8}O_{3-\delta}$, NexTech Materials Ltd., USA) powder was mixed with an organic solution and brush painted on the top surface of the electrolyte and sintered at 900 °C for 2 h in air. The active area of both the cathode and the anode was 3 mm^2. Pt paste (no. 6082, Engelhard, USA) was brush painted and subsequently Pt mesh (52 mesh, Alpha Aesar, USA) was attached to the sintered electrodes as a current collector at 850 °C for 1 h in air.

The cell was glass-sealed to an alumina tube for power testing. The cells were characterized at 700, 750 and 800 °C. A fuel gas of 97% H_2 + 3% H_2O was fed at a flow rate of 30 ml per min to the anode side and stationary air was used as the oxidant. An electrochemical interface (Solartron, SI 1287, UK) and an impedance analyzer (Solartron, SI 1260, UK) were used to obtain impedance spectra. The spectra were fitted using an analysis software (ZSimpWin, PerkinElmer Instruments, USA). Current versus cell potential was measured with an electrochemical interface (SI1287). The microstructure was observed with a field-emission scanning electron microscope (JEOL, model 3330F, Japan).

3. Results and discussion

Cross-sectional scanning electron micrographs of a single cell are presented in Fig. 2. As seen in Fig. 2a, the YSZ electrolyte film, sandwiched between a porous LSCF cathode (top layer) and a porous NiO–YSZ anode (bottom layer), is dense and ~16-μm thick. Although the cathode and the anode layers were brush painted, the variation in thickness is not large, namely 20–30 μm. Good adhesion is found between the electrolyte and electrodes. Comparison of the images in Fig. 2b and c shows that the NiO–YSZ anode has a much coarser particle size than the LSCF cathode. This is because the anode is sintered at a much higher temperature than the cathode (1300 °C versus 900 °C). The particle size of the anode is ~1 μm and that of cathode is ~0.3 μm.

In order to evaluate the contribution of ohmic and interfacial polarization resistances, the impedance of the cell was measured at 700, 750 and 800 °C under open-circuit conditions; the spectra are shown in Fig. 3. The ohmic resistance (R_{ohm}) and the polar-

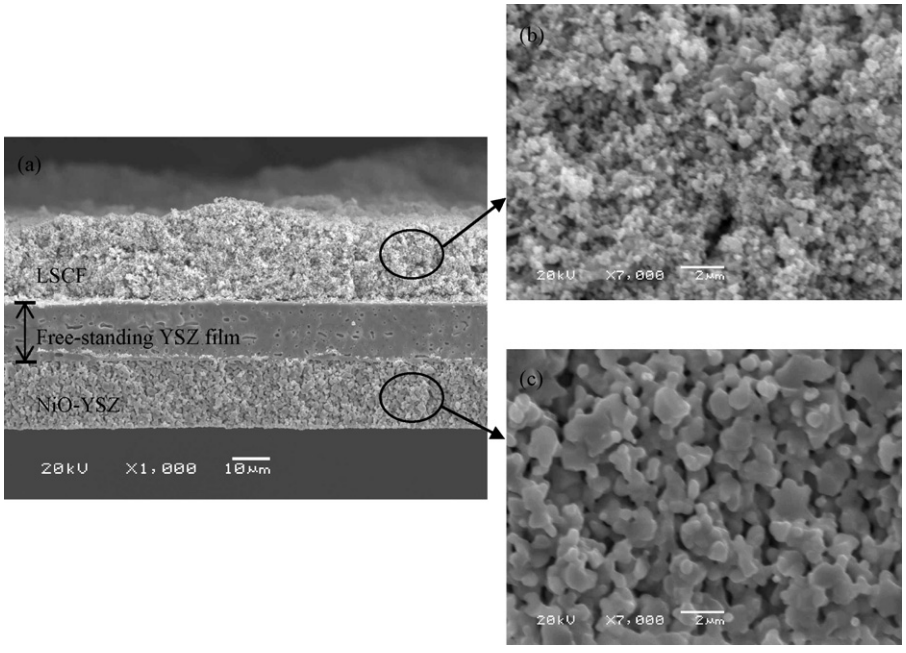

Fig. 2. Scanning electron micrographs of: (a) cross-section of thick-film YSZ supported cell with Ni–YSZ anode and LSCF cathode (bar = 10 μm); YSZ film is ~16 μm thick; (b) LSCF cathode (bar = 2 μm); (c) NiO–YSZ anode (bar = 2 μm).

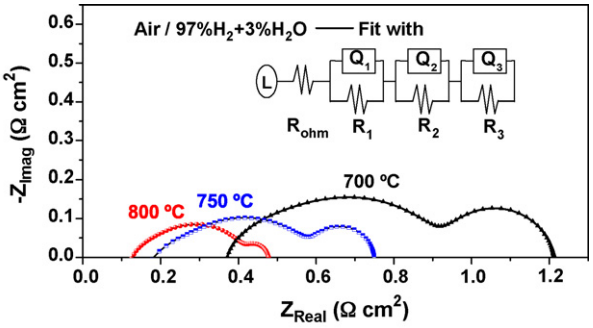

Fig. 3. Impedance spectra of thick-film YSZ-supported cell with Ni–YSZ anode and LSCF cathode. Impedance measured under open-circuit conditions at 700, 750 and 800 °C, respectively.

ization resistance (R_P) values of the cell were extracted from the impedance spectra. The impedance patterns show that the total resistance (R_{tot}) of the cell is determined primarily by R_p at all three temperatures. For example, the R_{ohm} value is ~0.12 Ω cm^2 and the R_p value is ~0.36 Ω cm^2. The contribution of R_{ohm} to the R_{tot} value is small due to the thinner (~16 μm) electrolyte layer. If the thickness of the electrolyte increases to 150–200 μm, as is generally employed in a conventional electrolyte-supported cell, the R_{ohm} value is expected to become ~10 times larger than the current value and thus dominate the R_P value. Thus the advantage of using a thinner (~16 μm) electrolyte layer is clearly demonstrated. The impedance spectrum is composed of three depressed semicircles or arcs. The spectra were fitted using the equivalent circuit shown in Fig. 3, where R_{ohm} is the ohmic resistance, L is the inductance, and the series connection of (R_1,Q_1), (R_2,Q_2) and (R_3,Q_3) corresponds to the three arcs, respectively. R_i is the resistance and Q_i is the constant-phase element. The R_{tot}, R_P and R_{ohm} values, as determined from the impedance spectra, are plotted as a function of temperature as shown in Fig. 4. The ratio of R_P to R_{tot} is ~75% at 800 °C and slightly decreases with decreasing temperature. This again confirms that the performance of the cell is limited by the R_P value. The activation energy (E_a) of R_{tot} (~0.92 ± 0.008 eV) is closer to that of R_P (~0.85 ± 0.006 eV) rather than that of R_{ohm} (~1.11 ± 0.13 eV). The E_a value of R_{ohm} obtained from the Arrhenius plots of R_{ohm}, 1.11 eV, is similar to the reported value (~1.07 eV) for the E_a value of 8YSZ grain or bulk conductivity [10]. Thus the R_{ohm} value consists mainly of the grain resistance of the electrolyte. Although the R_{ohm} value is smaller than the R_p value at the present test temperatures, it is expected that the former will increase more rapidly than the latter with decreasing temperature below 700 °C due to the larger E_a value of R_{ohm} than R_P. Further reduction of electrolyte thickness or adoption of a new material is required to

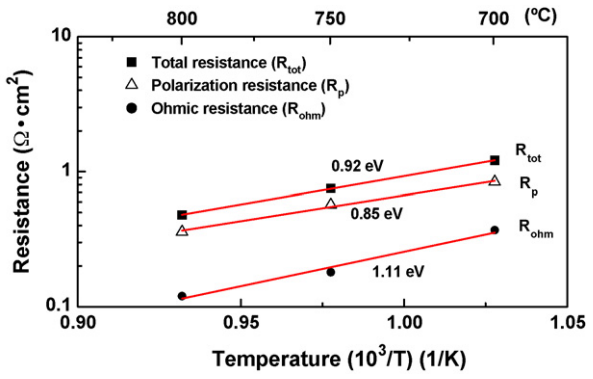

Fig. 4. Total resistance, polarization resistance and ohmic resistance determined from impedance plot and shown as function of temperature.

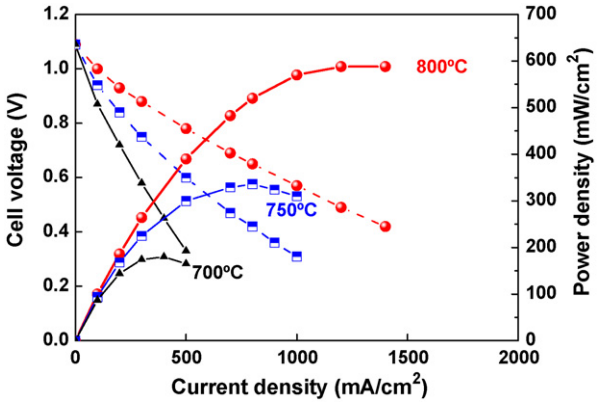

Fig. 5. I (current)–V (voltage) and I (current)–P (power) curves of test fuel cell at 700, 750, and 800 °C. 97% H_2 + 3% H_2O mixture used as fuel and air as oxidant.

decrease the R_{ohm} value for low-temperature use. Since the current cell performance is limited by the R_P value, it is expected that better cell performance can be achieved by further reduction of the R_P value. Examination of impedance spectra reveals that the R_P value is mostly determined by two arcs (R_2–Q_2, R_3–Q_3) in the low- and medium-frequency ranges. The size of the arc obtained in the high-frequency range (R_1–Q_1) is very small and thus the contribution to R_{tot} can be neglected. It is further found that the R_2 value is two to three times larger than the R_3 value. Thus the R_P value is determined mainly by the R_2 value at all three test temperatures. The E_a value of R_2 (~0.94 ± 0.06 eV) is also closer to that of R_P (~0.85 ± 0.006 eV) than that of R_3 (~1.10 ± 0.09 eV). A separate examination of cathodic and anodic R_P values under various thermodynamic conditions may be required to reduce the R_P value. The positioning of the reference electrode should also be considered.

The cell voltage and the corresponding power density are presented in Fig. 5 as a function of current density for a single cell characterized at 700, 750 and 800 °C. The open-circuit voltage (OCV) for 97% H_2 + 3% H_2O/air is ~1.09 V at 800 °C, which is very close to the theoretical value of 1.10 V at 800 °C. This indicates that the electrolyte film is quite dense with no pores or cracks. The founding also proves that good sealing is obtained between the electrolyte film and the YSZ ring. The maximum power density is 180, 340 and 590 mW cm^{-2} at 700, 750 and 800 °C, respectively. This result shows that high performance is achievable from an electrolyte-supported SOFC operating at 800 °C. The power densities are comparable with the performance (200–1900 mW cm^{-2} at 800 °C) of most anode-supported SOFCs with YSZ electrolytes [11–15]. It is expected that the operation temperature can be lowered further by using alternative electrolytes of higher ionic conductivity at lower temperature. For example, ceria or lanthanum gallate may be used as an electrolyte material. Although a relatively small-sized cell (~3 mm^2) has been tested in this study, a larger cell can be made by controlling the fabrication process. An array of cells can also be made by sintering many pieces of thick-film electrolyte (<20 μm) to pre-drilled holes in the supporting electrolyte sheet.

4. Conclusions

A thick-film electrolyte (thickness ~16 μm)-supported SOFCs has been successfully fabricated. A new experiment set-up, which utilizes a supporting ring for a thick-film electrolyte, enables power density measurements to be made for an electrolyte as thin as ~16 μm. Using LSCF as a cathode and Ni–YSZ as a composite anode, the cell with a YSZ thick-film electrolyte achieves a high performance, e.g., maximum power density of 590 mW cm^{-2} at 800 °C. This value is comparable with the performance of most

anode-supported SOFCs with YSZ electrolytes. It is also found that polarization resistance mainly limits cell performance, hence showing the advantage of the present approach. Consequently, it is expected that cell performance can be improved by reducing the polarization resistances. Low-temperature operation is also considered feasible by adopting alternative electrolyte materials.

Acknowledgement

Supported by POSTECH BSRI research fund-2007.

References

[1] N.Q. Minh, J. Am. Ceram. Soc. 76 (1993) 563–588.
[2] N.Q. Minh, T. Takahashi, Science and Technology of Ceramic Fuel Cell, Elsevier, NY, 1995, pp.147–161.
[3] A. Weber, E.I. Tiffée, J. Power Sources 127 (2004) 273–283.
[4] H. Tu, U. Stimming, J. Power Sources 127 (2004) 284–293.
[5] M. Cassidy, G. Lindsay, K. Kendal, J. Power Sources 61 (1996) 189–192.
[6] J. Will, A. Mitterdorfer, C. Kleinlogel, D. Peredins, L.J. Gaucker, Solid State Ionics 131 (2000) 79–96.
[7] S.C. Singhal, L. Kendall, High Temperature Solid Oxide Fuel Cells: Fundamentals, Design and Applications, Elsevier, NY, 2003, pp.197–228.
[8] J.M. Lee, G.M. Choi, J. Eur. Ceram. Soc. 27 (2007) 4219–4222.
[9] H.J. Cho, G.M. Choi, J. Power Sources 176 (2008) 96–101.
[10] J.H. Joo, G.M. Choi, Solid State Ionics 177 (2006) 1053–1057.
[11] S. Souza, S.J. Visco, L.C. De Jonghe, Solid State Ionics 98 (1997) 57–61.
[12] Y.J. Leng, S.H. Chan, K.A. Khor, S.P. Jiang, P. Cheang, J. Power Sources 117 (2003) 26–34.
[13] J. Kong, K. Sun, D. Zhou, N. Zhang, J. Mu, J. Qiao, J. Power Sources 117 (2003) 26–34.
[14] L. Zhang, S.P. Jiang, W. Wang, Y. Zhang, J. Power Sources 170 (2007) 55–60.
[15] S.D. Kim, H. Moon, S.H. Hyun, J. Moon, J. Kim, H.W. Lee, Solid State Ionics 178 (2007) 1304–1309.